Hindawi
International Journal of Polymer Science
Volume 2019, Article ID 9483127, 7 pages
https://doi.org/10.1155/2019/9483127

Research Article

In Vitro-In Vivo Correlation for the Degradation of Tetra-PEG Hydrogel Microspheres with Tunable β-Eliminative Crosslink Cleavage Rates

Jeff Henise,[1] **Shaun D. Fontaine**,[1] **Brian R. Hearn**,[1] **Samuel J. Pfaff**,[1] **Eric L. Schneider**,[1] **Julia Malato**,[2] **Donghui Wang**,[2] **Byron Hann**,[2] **Gary W. Ashley**,[1] **and Daniel V. Santi**[1]

[1]*ProLynx, 455 Mission Bay Blvd. South, San Francisco, CA 94158, USA*
[2]*Helen Diller Family Comprehensive Cancer Center University of California, San Francisco, 1450 3rd St., San Francisco, CA 94158, USA*

Correspondence should be addressed to Daniel V. Santi; daniel.v.santi@gmail.com

Academic Editor: Christopher Batich

The degradation of Tetra-PEG hydrogels containing β-eliminative crosslinks has been studied in order to provide an *in vitro-in vivo* correlation for the use of these hydrogels in our chemically controlled drug delivery system. We measured time-dependent gel mass loss and ultrasound volume changes of 13 subcutaneously implanted Tetra-PEG hydrogel microspheres having degradation times ranging from ~3 to 250 days. Applying a previously developed model of Tetra-PEG hydrogel degradation, the mass changes correlate well with the *in vitro* rates of crosslink cleavage and hydrogel degelation. These results allow prediction of *in vivo* biodegradation properties of these hydrogels based on readily obtained *in vitro* rates, despite having degradation times that span 2 orders of magnitude. These results support the optimization of drug-releasing hydrogels and their development into long-acting therapeutics. The use of ultrasound volume measurements further provides a noninvasive technique for monitoring hydrogel degradation in the subcutaneous space.

1. Introduction

We have developed a chemically controlled drug delivery system in which a drug is covalently attached via a carbamate to a polymeric hydrogel carrier using a self-cleaving β-eliminative linker (L1); a similar β-eliminative linker (L2) with a slower cleavage rate is installed into each crosslink of the polymer to trigger gel degradation after drug release (Figure 1). Upon subcutaneous injection, the drug is slowly released into the systemic circulation, and subsequently, the gel biodegrades into small fragments that are eliminated.

Figure 2 depicts the chemistry that drives linker cleavage for both drug release and gel biodegradation. Here, the linker is attached to a drug or polymer chain (carrier) *via* a carbamate group (Figure 2, 1). Two carbons removed from the carbamate leaving group is an acidic carbon–hydrogen bond (C–H) which also contains an electron-withdrawing "modulator" (Mod) group that controls the pK_a of the C–H bond. Upon proton removal to give 2 (in Figure 2), a rapid β-elimination occurs, cleaving the linker-carbamate bond and releasing the free drug. The rate of drug release is proportional to the acidity of the proton, which is, in large part, controlled by the electron-withdrawing ability of the pK_a modulator. The rate of linker cleavage is also retarded as the basicity of the amine in the carbamate increases [1] or by substitution of deuterium for hydrogen in the acidic C–H bond to obtain a primary kinetic isotope effect [2].

The polymeric carrier we use is the well-studied, near-homogeneous Tetra-PEG hydrogel [3] that can be administered by subcutaneous (SC) in situ gelation [1, 4] or, preferably, by SC injection of uniform ~40 μm-diameter microspheres through a small-bore needle [5].

Most long-acting drug delivery systems involve encapsulation of a drug in a polymer that contains ester or other

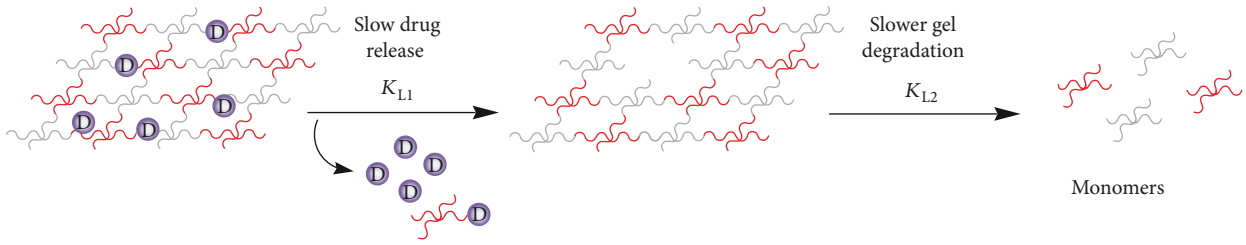

Figure 1: Depiction of chemically controlled drug release and subsequent degradation of a Tetra-PEG hydrogel with β-eliminative crosslinks.

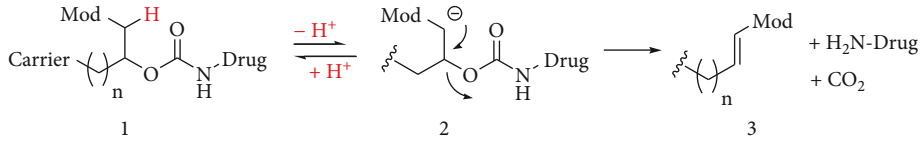

Figure 2: β-Elimination mechanism of linker cleavage.

hydrolysable crosslinks, as exemplified by PLGA delivery systems. Here drug release and polymer degradation/erosion occur concurrently. In the present system, the rates of drug release, k_{L1}, and hydrogel degradation, k_{L2}, are independent and can be balanced so that the drug is released before the gel undergoes significant degradation/erosion. Otherwise, excessive fragments of gel will be solubilized that are covalently bound to the drug; although the drug will ultimately be released, such transient fragments should be minimized. Nonetheless, polymer degradation should be as fast as practical, so the gel does not remain in an *in vivo* compartment as an inert substance for unnecessary periods. This goal requires coordination and balancing of the rates of hydrogel degradation and drug release; we have suggested from computational approaches that the ratio of rates k_{L2}/k_{L1} of ~3 may be a desirable balance for most such subcutaneous implants [6].

While the *in vivo* k_{L1} can be determined by pharmacokinetic studies of the released drug, the *in vivo* rate of gel degradation k_{L2} is more difficult to assess. Temporal profiles describing mass loss or erosion of SC-implanted gels have conventionally been measured by analysis of the remaining implanted material in excised tissue from animals over time. Such studies have usually been performed by analysis of one implant per animal after euthanasia, necessitating multiple animals for each profile. Recently, efforts have shifted to the use of biomedical imaging to noninvasively monitor *in vivo* changes accompanying degradation of implants—notably MRI and various ultrasound (US) methodologies that can be translated across species [7]. However, these approaches measure several concurrent changes, including mass loss and gel swelling or shrinkage. Regardless of the methodology used, *in vitro* models have thus far been poor predictors of *in vivo* gel degradation.

In the present work, we first established an approach to assess the mass loss of degradable β-eliminative Tetra-PEG hydrogel microspheres subcutaneously (SC) implanted into rats. Temporal monitoring of volume changes were likewise determined using 3D ultrasound computer tomography (USCT) measurements of the implant cavity volumes. Then, we used these methods to determine degradation profiles of Tetra-PEG hydrogel microspheres having *in vivo* degradation times ranging from ~3 to 250 days. We fit the *in vivo* mass loss profiles to our mechanistic model for Tetra-PEG hydrogel degradation [6], relating them to the *in vitro* rates of microsphere degelation. These equations allowed translation of easy-to-obtain *in vitro* data to predict *in vivo* biodegradation rates, thus providing *in vitro-in vivo* correlations (IVIVC). Finally, we established a correlation between hydrogel degradation and implant volume at the injection site as measured by ultrasound which allows for noninvasive monitoring.

2. Materials and Methods

2.1. Synthesis and Crosslink Structure of Hydrogels. The fabrication of our Tetra-PEG hydrogel drug delivery system has been described [4, 5] and is detailed in Supplementary Material. Two general types of hydrogels were prepared, one where the cleavable crosslinker is attached to the α-group of lysine and the other where the crosslinker is attached to the ε-group of lysine (Figure 3). The hydrogels in Figure 3 were prepared by combining a 20 kDa 4-armed PEG-(cyclooctyne)$_4$ (4) with a 20 kDa 4-armed PEG-(azido-linker-lysine)$_4$ where the crosslinker (L2) is attached to either the α- (5) or ε-amine (6) of the lysine to give the corresponding α- (7) or ε- (8) triazolyl-crosslinked hydrogels. The free lysine amino groups of the hydrogels were then modified with 0.2 equivalents of 5(6)-carboxyfluorescein to serve as a probe for degradation, and the excess amines were capped by acetylation with acetyl N-hydroxysuccinimide. For comparison, hydrogel materials were prepared both as bulk-gel cones and as microspheres.

2.2. Measurement of In Vitro Gel Properties. Values for the crosslinker cleavage half-life ($t_{1/2,L2\,in\,vitro}$) for α-amine crosslinks (7) were measured by observing the decomposition of MeO-PEG-linker-carbamoyl-[5-(aminoacetamido)-fluorescein] as previously reported [1], while those for ε-linked crosslinks (8) were measured using PEGylated Nα-(2,4-dinitrophenyl)-Nε-(carbamoyl-linker)-lysine as previously reported [1]. The *in vitro* degradation or time to reverse degelation (t_{RG}) of the hydrogels was determined by placing fluorescein-labeled hydrogels, as cones or as microspheres,

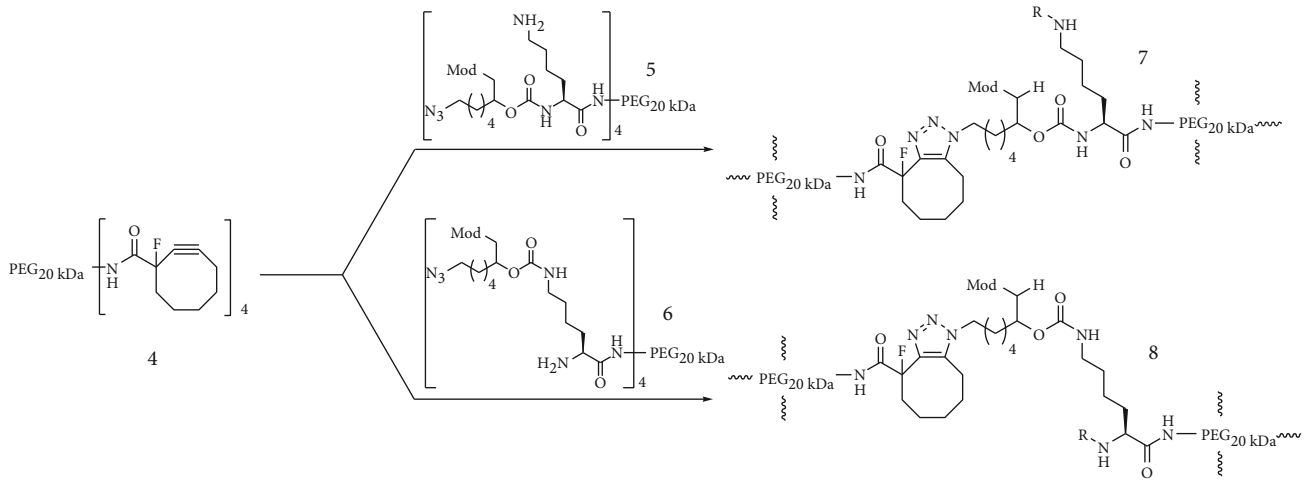

Figure 3: Formation of Tetra-PEG hydrogels with cleavable crosslinks connected to the α- or ε-amine of a lysine residue that forms part of the crosslink. The R groups in hydrogels 7 and 8 show the position where a cleavable linker can be attached to tether a releasable drug or, in the case of this work, where fluorescein has been attached to facilitate detection of gel components by fluorescence upon gel degradation.

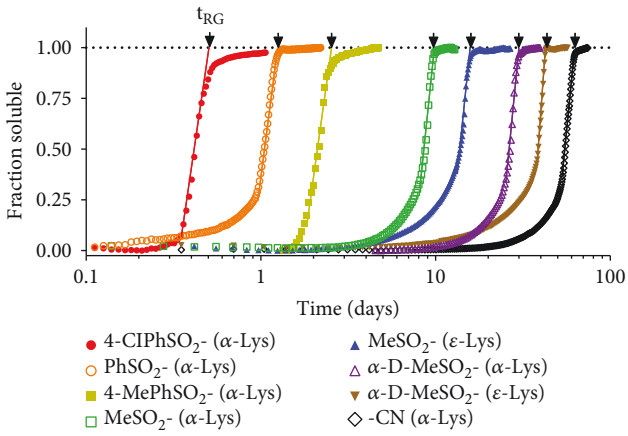

Figure 4: *In vitro* solubilization (degelation) curves of Tetra-PEG hydrogels with crosslinks of different cleavage rates showing t_{RG} values (Table S1). Crosslink cleavage rate modulators are shown in the legend of the figure. The t_{RG} values were determined as an average of four replicates under accelerated conditions of pH 8.4, 9.0, or 9.4 at 37°C and converted to pH 7.4 values as described [11].

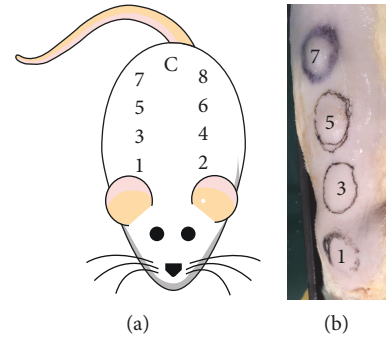

Figure 5: Injections of microspheres in the rat. (a) Temporal sequence of eight injections of microspheres in the rat spaced in intervals of approximately $(3 \times t_{RG\,in\,vitro})/8$; C is an untreated control site for background fluorescence determination. (b) Photograph of tattoo-marked SC injection sites labeled 1, 3, 5, and 7 at termination of the experiment where 1 is the oldest injection with almost completely degraded microspheres and 7 is the newest injection with fully intact microspheres. Tattoo circles are approximately 12 mm in diameter.

into buffer at 37°C and following the dissolution of gel components by absorbance at 495 nm (Supplementary Material). The t_{RG} is determined as the time of intersection of the steepest part of the *in vitro* solubilization curve with the horizontal line representing total solubilization (Figure 4).

2.3. In Vivo Gel Erosion and Volume Changes. For each gel, subcutaneous injections of fluorescein-labeled microspheres (100 μL) were made at various times into 8 sites spaced evenly over the shaved back of rats (Figure 5(a)). Three replicate animals were used for each gel. The time interval between injections was calculated as approximately $(3 \times t_{RG\,in\,vitro})/8$, so that the eight injections were spaced in time to cover the expected period for complete degradation [6]. In this manner, the earliest injections had the longest residence time in the animal and the latest injections had the shortest residence time. After an animal had received seven injections (Figure 5(b)), and the first injection could no longer be detected by palpation, the animal was administered the final injection, at time equal to approximately $3 \times t_{RG\,in\,vitro}$, then was euthanized. Each injection site was analyzed for implant volume by 3D ultrasound computer tomography (USCT), and then the tissue surrounding the injection sites was removed using a 12 mm punch biopsy for measurements of the remaining gel by digestion of tissue followed by fluorescein detection. These methods are described in detail in Supplementary Material.

3. Results and Discussion

3.1. Synthesis and Crosslink Structure of Hydrogels. While the rate of cleavage of our β-eliminative linkers is primarily

controlled by the structure of the modulator group as discussed above, this rate can be fine-tuned using various structural parameters, including the nature of the releasable amine group to which the linker is attached (e.g., the α- or ε-amino group of lysine) and the use of a deuterium atom in place of the acidic hydrogen atom shown in Figure 2 to slow the cleavage via a kinetic isotope effect [1, 2]. Using this information, a series of 13 Tetra-PEG hydrogels was prepared, covering a range of *in vitro* degelation times from 12 to 2750 hours (Supplementary Material (available here)).

3.2. Correlation between Linker Cleavage Rate and In Vitro Time to Reverse Degelation (t_{RG}). The t_{RG} is the time at which the initially intact crosslinks are reduced to a critically low fraction and the gel becomes completely soluble. For Tetra-PEG hydrogels, the t_{RG} is dependent upon the half-life of crosslink bond cleavage ($t_{1/2,L2}$) and the quality of the gel (f) as defined by the number of unformed crosslinks present in the initial gel as shown below [6, 8]:

$$t_{RG} = t_{1/2,L2} \cdot \frac{\ln((1-f)/0.39)}{\ln(2)}, \quad f = 1 - 0.39 \cdot 2^{t_{RG}/t_{1/2,L2}}. \tag{1}$$

Conversely, if $t_{1/2,L2\,in\,vitro}$ is known from kinetic measurements of the crosslinking group, and $t_{RG\,in\,vitro}$ is known from *in vitro* degelation measurements, the gel quality factor f can be calculated as shown. Supplementary Material, Table S1, provides the t_{RG}, $t_{1/2,L2\,in\,vitro}$, and f values of all hydrogels used in this study. Calculation of the quality factors revealed that the hydrogels fell into one of two groups, a major group (Table S1, D-M) having $f \sim 0.20 \pm 0.08$ and a small group (Table S1, A-C) having $f \sim 0.45 \pm 0.02$. The difference in these groups was traced to the quality of the starting commercial PEG-tetraamines used to synthesize the gels. Groups D-M were prepared using a PEG-tetraamine having 98% of expected amine end groups, while groups A-C were prepared using a PEG-tetraamine having only 82% of expected amine end groups. Thus, gels A-C contained a far greater fraction of unformed crosslinks in the initial gels.

Within experimental error, the t_{RG} of 100 μL single-molecule bulk-gel cones are the same as for the $\sim 4 \times 10^{-5}$ μL microspheres (Table S1), showing that degradation rates of gels are volume independent. Also, since the surface area to volume ratio of microspheres are ~100-fold higher than the cones, the data show that linker cleavage rates are homogeneous throughout the gels, making t_{RG} independent of gel particle size.

As predicted, attachment of the crosslinker to the more basic ε-amine rather than α-amine groups of Lys slows both the β-elimination reaction and the t_{RG} of gels by ~2-fold [1]. Likewise, an α-deuterated linker with Mod = $MeSO_2-$ or -CN shows an α-deuterium isotope effect that slows both the β-elimination and the t_{RG} of gels by ~2.5- to 3.5-fold, respectively [2].

3.3. In Vivo Gel Erosion and Volume Changes. Each hydrogel microsphere material was injected into the subcutaneous space of rats in a sequence temporally spaced according to the expected degelation time, as described in Materials and Methods, in order to get a time course of *in vivo* degelation (Figure 5(a)). The resultant circular to slightly elliptical protuberances from the 100 μL injections were initially ~10 mm (L) × ~8 mm (W) × ~3 mm (h). With time, the protuberances decreased in size, appeared to flatten, and then disappeared (Figure 5(b)).

Measurements of the hydrogel components remaining in each injection site were made by excision of tissue containing the microspheres and detection of fluorescein by fluorescence following digestion of the tissue as described in Material and Methods. During degradation of the hydrogel, cleavage of the crosslinks results in formation of oligomeric pieces of gel of various sizes; if the oligomer is sufficiently small, it will be eliminated from the subcutaneous space through the systemic or lymphatic circulation. The mass of gel remaining at the injection site will equal the original mass minus the mass of released small fragments. This analysis measures the remaining mass of intact microspheres as well as any large soluble fragments that have not diffused beyond the perimeter of the sampled tissue.

According to our mechanistic model for Tetra-PEG hydrogels [6], the probability ($P_{N,t}$) that an oligomeric gel fragment composed of N monomers is released from the gel at time t is given as

$$P_{N,t} = \sum Q_{NLD} p_t^{N-1+L} q_t^{2N+2-(2L+D)}, \quad p_t = (1-f) * \exp(-k_2 t), q_t = 1 - p_t, \tag{2}$$

where k_2 is the first-order rate constant for crosslink cleavage ($k_2 = \ln(2)/t_{1/2,L2}$), f is the gel quality factor (equation (1)), and Q_{NLD} is a statistical factor describing the number of oligomers of size N having a topology described by L and D that contain a given monomer as detailed in [6]. If we set an upper limit of N_{max} for the size of gel fragments that can be efficiently eliminated from the SC space, the fraction of the total gel released at time t is thus given by the sum of the probabilities of release for $N \le N_{max}$, and the mass of remaining hydrogel (Gel_t/Gel_0) can be calculated as

$$\frac{Gel_t}{Gel_0} = 1 - \sum_{N=1,N_{max}} \left\{ \sum Q_{NLD} p_t^{N-1+L} q_t^{2N+2-(2L+D)} \right\}. \tag{3}$$

According to this model, the degradation behavior of the hydrogel should be determined solely by the rate of cleavage of crosslink bonds (k_2) and the gel quality factor f. According to our model, then, any Tetra-PEG hydrogel having quality factor f should exhibit the same time course for mass of gel remaining at the injection site when the time axis is normalized as $t/t_{RG\,in\,vitro}$.

For analysis, the fluorescence remaining at the injection site at time t ($F_{(t)}$) was normalized to the value at $t = 0$ ($F_{(t)}/F_0$) and is equal to Gel_t/Gel_0 (equation (3)). The time of the measurements was also normalized to t_{RG} ($t/t_{RG\,in\,vitro}$)

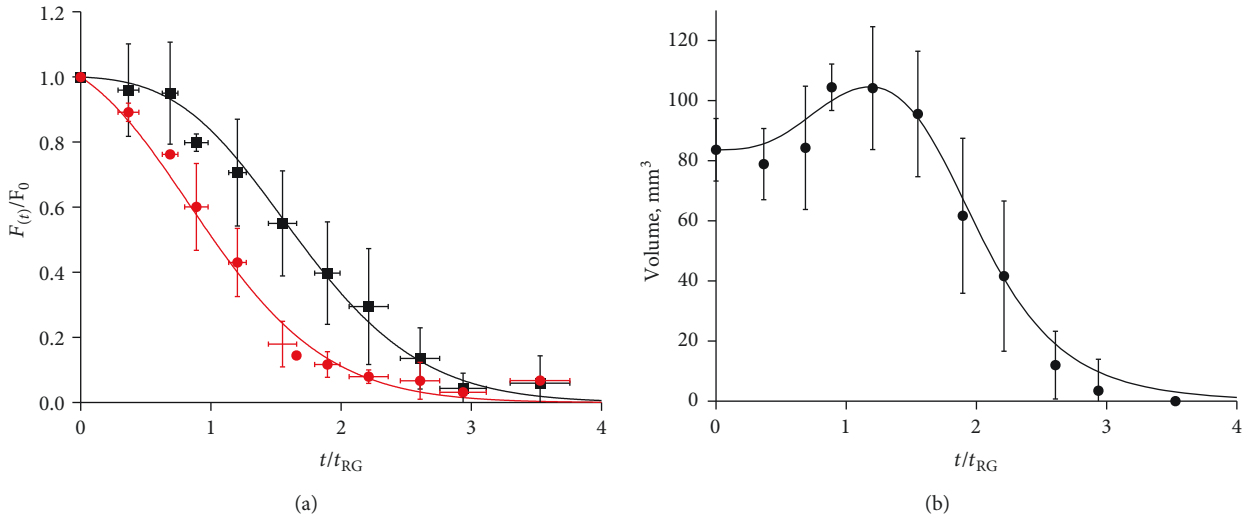

FIGURE 6: Loss of gel components as a function of t_{RG}. (a) Fractional fluorescence ($F_{(t)}/F_0$) remaining at the injection site as a normalized function of $t/t_{RG\,in\,vitro}$ for 13 different hydrogel microspheres having t_{RG} values ranging from 12 to 2750 hours and $f = 0.21$ (black square) or $f = 0.45$ (red circle). The data were grouped into clusters having a median of $t/t_{RG\,in\,vitro} \pm 0.2$, and vertical lines show the mean ± standard deviation of the measured parameter within each cluster. Theoretical curves were calculated according to equation 3 where $N_{max} = 6$ and $t_{1/2,L2} = 1.36 \cdot t_{RG\,in\,vitro}$. (b) Fit of the clustered ultrasound volumes of materials E-M (Table S1) to equation 4 using $V_0 = 83.5$ mm^3 and $Q = 1.5$. Error bars represent the standard deviation of the clustered volume data.

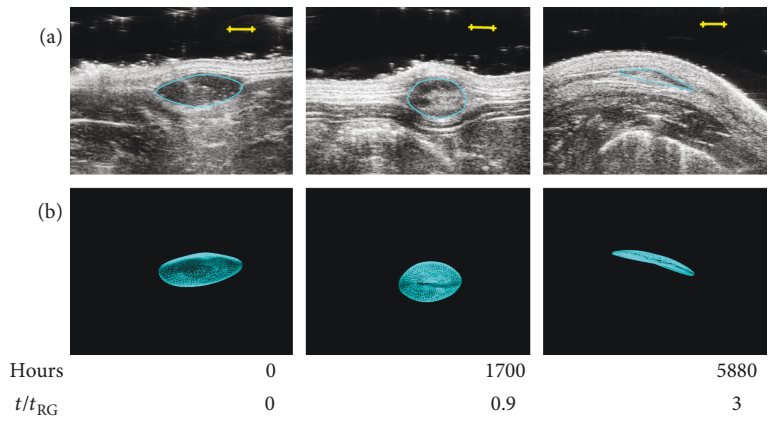

FIGURE 7: Ultrasound analysis of implants. (a) 2D images of microsphere implants, with the degradation crosslink modulator -CN (ε-Lys), showing the widest cross-section at 0, 1700, and 5880 hours post injection, and the time relative to *in vitro* reverse degelation time ($t/t_{RG\,in\,vitro}$). Scale bars = 2 mm. (b) 3D USCT renderings showing the volumes of the implants shown in (a).

for a given material. Data sets from materials of equivalent quality factor f were then overlaid (Figure 6(a)). This revealed that the loss of gel mass from the injection site followed identical behavior for all gel materials having equivalent quality factors despite having residence times that varied by an order of magnitude and that the initial quality of the gel has a profound impact on the *in vivo* degradation behavior. Regardless of the quality factor, the best-fit values for $t_{1/2,L2\,in\,vivo}$ were uniformly longer than expected by a factor of 1.36 based on the values ($t_{1/2,L2\,in\,vitro}$) measured *in vitro* at 37°C, suggesting that the *in vivo* t_{RG} is ~1.36 times the measured *in vitro* rate. This is consistent with the reported lower subcutaneous temperature in rats relative to the core temperature of 37°C [9]. Using the previously reported temperature dependence for linker cleavage [1], this suggests that the temperature in the rat subcutaneous space is approximately 34°C.

The amount of hydrogel remaining at the subcutaneous injection site over time is thus directly predictable based on our previously developed mechanistic model of Tetra-PEG hydrogel degradation, requiring knowledge only of their *in vitro* t_{RG} values and linker cleavage rates.

As tissue biopsy is not a desirable means of studying hydrogel residence in a clinical setting, we measured the volume occupied by hydrogel implants by 3D ultrasound computer tomography (USCT), a painless, noninvasive technique readily translated to other animals and humans. Figure 7 shows that immediately after injection of microspheres, a cross-section of the cavity formed in the SC space is as an elliptical structure readily identified by its unique

sonographic features. Initially, the implanted hydrogel displays contrasting echogenic elements which over time transforms to an echolucent space that decreases in volume until it is undetectable. The volumes occupied by the microspheres were determined by integration of the implant area from 2D ultrasound image stacks obtained at constant depth and evenly spaced intervals (0.5 mm) along the length of the implant to give a 3D model of the implant (Figure 7(b)). Plots of cavity volume vs. time were constructed for each gel studied (Figure S1).

The volume change over time was more complex than that for the loss of hydrogel components described above due to the swelling behavior of the hydrogels as they degrade and the force applied by the surrounding tissues [10]. As crosslinks are broken, the gel structure becomes less dense and the gel occupies a larger equilibrium volume up until the point that mass loss from the gel is sufficient to overcome the decrease in density. It is further expected that there will be some pressure applied by the surrounding tissues to counter increases in gel volume due to this swelling. Given this added complexity, only hydrogels having equivalent quality factors ($f = 0.2$) were included in the volume analysis. Data points between materials were combined into the same groups of equivalent $t/t_{\mathrm{RG\,in\,}vitro} \pm 0.2$ described above for the fluorescence data. The average initial cavity volumes in all animals of groups E-M (Table S1) resulting from 100 μL injections were 84 ± 15 mm^3, probably reflecting compression of the suspension and rapid absorption of the liquid buffer surrounding the microspheres. After an initial period, gel swelling became evident with the average volume increasing to 104 ± 36 mm^3 at a time equal to the *in vivo* t_{RG} (i.e., 1.36 times the *in vitro* t_{RG} as discussed above), after which the volume decreased to zero at 3-4 times the *in vitro* t_{RG}. The time required for the cavity to collapse was thus the same as the time at which gel components were completely lost (Figure 6).

In the absence of an analytical model for the change of hydrogel density during degradation, the ultrasound-determined volumes of the gels were empirically fit to a double-sigmoid curve (equation (4)) using parameters for initial volume V_0 and a swelling factor Q that describes the volume increase due to loss of gel density during degradation.

$$V_t = V_0 \left\{ \frac{1-Q}{\left(1 + \left(t/t_{\mathrm{RG\,in\,}vitro}\right)^3\right)} + \frac{Q}{\left(1 + \left(t/t_{\mathrm{RG\,in\,}vitro}\right)^6\right)} \right\}. \quad (4)$$

As for the fluorescence data described above, the cavity volumes measured by ultrasound predictably correlate with the *in vitro* properties of the hydrogels, allowing for the use of noninvasive ultrasound techniques to monitor the status of hydrogels in the subcutaneous space.

The primary objectives of this work were to characterize the *in vivo* degradation rates of Tetra-PEG hydrogel microspheres containing tunable β-eliminative crosslinks and to construct an *in vitro-in vivo* correlation (IVIVC) that would allow prediction of *in vivo* degradation from data obtained *in vitro*. Using microspheres with *in vivo* degradation times of ~3 to 250 days, we measured the loss of gel mass over time from the injection site and demonstrated that the *in vivo* degradation behavior is well-described by the mechanistic model of Reid et al. [6]. Thus, the *in vivo* degradation behavior of our β-eliminatively linked Tetra-PEG hydrogels is predictable based only on the *in vitro* linker cleavage rate ($k_{\mathrm{L2\,in\,}vitro}$) and hydrogel degelation time ($t_{\mathrm{RG\,in\,}vitro}$). Importantly, the relationship held for 13 different gels spanning a $t_{\mathrm{RG\,in\,}vitro}$ range of 12 to 2750 hours and should be useful for predicting *in vivo* properties of yet-unmade gels. In a secondary objective, we demonstrated that changes in volume of the subcutaneous microsphere depots as measured by ultrasound imaging are an effective, noninvasive, and painless surrogate for following *in vivo* degradation of our hydrogels.

Approaches for measuring actual mass loss accompanying gel degradation usually involve isolation (excision) and quantitation of remaining material in animal implants over time. Early serial studies usually used one implant per animal and suffered from the need for numerous animals and interanimal variation. Here, the experimental design used longitudinal subcutaneous injections of the polymer at eight locations on a rat over the expected *in vivo* lifetime; then, after the first-injected polymer had disappeared by visualization/palpation, the animals were euthanized and the gels in all injection sites were analyzed. The earliest injections had the longest residence time in the animal, and the latest injections had the shortest residence time. Hence, a single animal provided the full temporal analysis of *in vivo* gel degradation, and intra-animal variation was avoided.

The constant gel mass over varying long periods prior to the onset of degelation shows that the microspheres do not migrate from the initial site of deposition. Thus, in case the microsphere-drug conjugates require removal, they can be completely excised by a simple punch biopsy.

4. Conclusions

In summary, we have characterized the *in vivo* degradation behaviors of Tetra-PEG hydrogel microspheres containing tunable β-eliminative crosslinks. Using Tetra-PEG hydrogel microspheres with *in vivo* degradation times of up to almost one year, we measured the time-dependent loss of gel substance from the injection site and the changes in volume of the injected microsphere depots in the subcutaneous compartment of rats. The *in vivo* loss of hydrogel from the injection site is completely predictable based on a mechanistic model and depends only on two parameters, the crosslinker cleavage rate ($k_{\mathrm{L2\,in\,}vitro}$) and the time to reverse degelation ($t_{\mathrm{RG\,in\,}vitro}$), that are readily measured *in vitro*. We have further developed a painless, noninvasive method for following the *in vivo* degradation of microsphere hydrogel depots involving ultrasound imaging.

Data Availability

The raw ultrasound images, measured fluorescein values, and raw *in vitro* degelation data used to support the findings of this study are available from the corresponding author upon request.

Conflicts of Interest

The authors declare that there are no conflicts of interest regarding the publication of this paper.

Acknowledgments

This work was supported in part by NSF grant 1429972.

Supplementary Materials

Supporting information is available and contains experimental procedures for the synthesis of hydrogel components, preparation of hydrogel microspheres, and *in vitro* and *in vivo* characterization of gel degradation. Also included are plots of raw *in vivo* data and a table of experimentally determined parameters. *(Supplementary Materials)*

References

[1] D. V. Santi, E. L. Schneider, R. Reid, L. Robinson, and G. W. Ashley, "Predictable and tunable half-life extension of therapeutic agents by controlled chemical release from macromolecular conjugates," *Proceedings of the National Academy of Sciences of the United States of America*, vol. 109, no. 16, pp. 6211–6216, 2012.

[2] B. R. Hearn, S. D. Fontaine, S. J. Pfaff et al., "Primary deuterium kinetic isotope effects prolong drug release and polymer biodegradation in a drug delivery system," *Journal of Controlled Release*, vol. 278, pp. 74–79, 2018.

[3] H. Kamata, X. Li, U. I. Chung, and T. Sakai, "Design of hydrogels for biomedical applications," *Advanced Healthcare Materials*, vol. 4, no. 16, pp. 2360–2374, 2015.

[4] J. Henise, B. R. Hearn, G. W. Ashley, and D. V. Santi, "Biodegradable tetra-PEG hydrogels as carriers for a releasable drug delivery system," *Bioconjugate Chemistry*, vol. 26, no. 2, pp. 270–278, 2015.

[5] E. L. Schneider, J. Henise, R. Reid, G. W. Ashley, and D. V. Santi, "Hydrogel drug delivery system using self-cleaving covalent linkers for once-a-week administration of exenatide," *Bioconjugate Chemistry*, vol. 27, no. 5, pp. 1210–1215, 2016.

[6] R. Reid, M. Sgobba, B. Raveh, G. Rastelli, A. Sali, and D. V. Santi, "Analytical and simulation-based models for drug release and gel degradation in a tetra-PEG hydrogel drug-delivery system," *Macromolecules*, vol. 48, no. 19, pp. 7359–7369, 2015.

[7] H. Zhou, M. Goss, C. Hernandez, J. M. Mansour, and A. Exner, "Validation of ultrasound elastography imaging for nondestructive characterization of stiffer biomaterials," *Annals of Biomedical Engineering*, vol. 44, no. 5, pp. 1515–1523, 2016.

[8] P. J. Flory, *Principles of Polymer Chemistry*, Cornell University press, Ithaca, 1953.

[9] A. D. O. Teixeira, C. N. Martins, A. M. V. d. Silva, A. M. Tozetti, R. D. M. Plentz, and L. U. Signori, "Temperature of cutaneous and subcutaneous tissue during the application of aerosols in rats," *Acta Scientiarum Health Sciences*, vol. 36, no. 2, p. 235, 2014.

[10] X. Li, Y. Tsutsui, T. Matsunaga, M. Shibayama, U. Chung, and T. Sakai, "Precise control and prediction of hydrogel degradation behavior," *Macromolecules*, vol. 44, no. 9, pp. 3567–3571, 2011.

[11] G. W. Ashley, J. Henise, R. Reid, and D. V. Santi, "Hydrogel drug delivery system with predictable and tunable drug release and degradation rates," *Proceedings of the National Academy of Sciences of the United States*, vol. 110, no. 6, pp. 2318–2323, 2013.

In vitro-in vivo correlation for the degradation of Tetra-PEG hydrogel-microspheres with tunable β-eliminative crosslink cleavage rates

Jeff Henise [1], Shaun D. Fontaine [1], Brian R. Hearn [1], Samuel J. Pfaff [1], Eric L. Schneider [1], Julia Malato [2], Donghui Wang [2], Byron Hann [2], Gary W. Ashley [1], Daniel V. Santi [1,*]

[1] ProLynx, 455 Mission Bay Blvd. South, Suite 145, San Francisco, CA 94158
[2] Helen Diller Family Comprehensive Cancer Center University of California, San Francisco, California, 1450 3rd St., San Francisco, CA 94158

Supporting Information

Table of Contents

I. General

PEG_{20kDa}-$(NH_2)_4$ was purchased from either NOF (PTE-200PA) or JenKem (A7026). Activated succinimidyl carbonate linkers were prepared as previously described [1]. All other reagents were reagent grade. Azide content was quantified by DBCO titration as previously described [2]. HPLC analyses were performed using an Agilent Series 1100 system equipped with a Jupiter 5 μm C_{18} column (150 x 4.6 mm), an Agilent G1329A autosampler, an Agilent G1315A

photodiode-array detector, and an Alltech 3300 ELSD. Products were eluted with a 10 min linear gradient of 20%-80% acetonitrile (0.1% TFA) in water (0.1% TFA) at a flow rate of 1 mL/min. LCMS analyses were obtained at the UCSF Small Molecule Discovery Center core facility using a Waters Micromass ZQTM equipped with a Waters 2795 Separation Module and a Waters 2996 Photodiode Array Detector. In vitro reverse gelation experiments were performed on a Hewlett-Packard 8453 UV-Vis spectrophotometer equipped with a water-jacketed multi-sample compartment fitted with a magnetic stirred [3].

II. Synthesis

1. Prepolymer A

1.A. α-Amino linked Lys-Prepolymer A: [N_3-L(Mod)-Lys(NH_2)-NH]$_4$-PEG_{20kDa}. The following is representative of procedures used for prepolymer A synthesis starting from H-Lys(Boc)OH in which the linker carbamate involves the α-amine of Lys.

Step 1. *N^{α}-(7-Azido-1-methylsulfonyl-2-heptyloxycarbonyl)-N^{ε}-Boc-Lys-OH*. A suspension of H-Lys(Boc)-OH (72 mg, 0.29 mmol) in 0.79 mL H_2O was successively treated with 1 M aq NaOH (0.29 mL, 0.29 mmol), 1 M aq $NaHCO_3$ (0.27 mL, 0.27 mmol), and a 0.2 M solution of *O*-(7-azido-1-methylsulfonyl-2-heptyl)-*O'*-succinimidyl carbonate (100 mg, 0.266 mmol, 0.1 M final concentration) in 1.35 mL of MeCN. After stirring for 1 h at ambient temperature, the reaction was judged to be complete by C18 HPLC (ELSD). The reaction mixture was partitioned between 40 mL of 1:1 EtOAc:$KHSO_4$ (5% aq). The layers were separated, and the aqueous phase was extracted with 20 mL of EtOAc. The combined organic layer was successively washed with water and brine (20 mL each). The organic phase was dried over $MgSO_4$, filtered, and concentrated to provide the crude intermediate carboxylic acid (124 mg, 0.244 mmol, 92% crude yield) that was used in its entirety in the next step.

Step 2. *N^{α}-(7-Azido-1-methylsulfonyl-2-heptyloxycarbonyl)-N^{ε}-Boc-Lys-OSu*. DCC (60% in xylenes, 2.6 M, 0.12 mL, 0.32 mmol) was added to a solution of *N^{α}*-(7-azido-1-methylsulfonyl-2-heptyloxycarbonyl)-*N^{ε}*-Boc-Lys-OH (124 mg, 0.244 mmol, 0.1 M final concentration) and *N*-hydroxysuccinimide (36 mg, 0.32 mmol) in 2.4 mL of CH_2Cl_2. After stirring at ambient temperature for 1 h, the reaction mixture was filtered through a cotton plug, and the filtrate was loaded onto a SiliaSep 4 g column. Product was eluted with a step-wise gradient of acetone in hexane (0%, 10%, 20%, 30%, 40%, 50%, 30 mL each). Clean product-containing fractions were combined and concentrated to provide the title compound (124 mg, 0.205 mmol, 77% yield, two steps) as a white foam. LC-MS, two diastereomers (*m/z*): calc, 627.2; obsd, 627.1 $[M+Na]^+$ and calc, 505.2; obsd, 505.0 $[M\text{-}Boc+H]^+$.

Step 3. *[N^{α}-(7-Azido-1-methylsulfonyl-2-heptyloxycarbonyl)-N^{ε}-Boc-Lys]$_4$-PEG_{20kDa}*. PEG_{20kDa}-$(NH)_4$ (250 mg, 12.5 μmol, 50.0 μmol NH_2, 0.02 M NH_2 final concentration) was dissolved in 1.25 mL of MeCN. A solution of *N^{α}*-(7-Azido-1-methylsulfonyl-2-heptyloxycarbonyl)-*N^{ε}*-Boc-Lys-OSu (39 mg, 65 μmol) in 1.25 mL of MeCN was added. The reaction was stirred at ambient temperature and analyzed by C18 HPLC (ELSD). The starting material was converted to a single product peak via three slower eluting intermediate peaks. After 45 min, Ac_2O (4.7 μL, 50 μmol) was added. The reaction mixture was stirred 30 min more then concentrated to ~1 mL by rotary evaporation. The product was precipitated by addition of the reaction concentrate to 25 mL of stirred MTBE. After triturating and incubating on ice for 30 min, the suspension was centrifuged (3000g, 4°C, 2 min), and the supernatant was decanted. The precipitate was washed with MTBE (2 x 25 mL), and the supernatants were decanted. Residual volatiles were

removed under vacuum to provide the title compound (255 mg, 11.6 μmol, 93% yield) as a white powder.

Step 4. *[N^{α}-(7-Azido-1-methylsulfonyl-2-heptyloxycarbonyl)-Lys]$_4$-PEG$_{20kDa}$*. TFA (1.3 mL) was added to a solution of [N^{α}-(7-azido-1-methylsulfonyl-2-heptyloxycarbonyl)-N^{ε}-Boc-Lys]$_4$-PEG$_{20kDa}$ (255 mg, 11.6 μmol, 100 mg/mL final concentration) in 1.3 mL of CH_2Cl_2. The reaction was stirred at ambient temperature and analyzed by C18 HPLC (ELSD). The starting material was converted to a single product peak via three faster eluting intermediate peaks. After 45 min, the reaction mixture was concentrated to dryness, and the resulting oil was triturated with 20 mL Et_2O. After incubating on ice for 30 min, the suspension was transferred to a 50 mL Falcon tube and centrifuged (3000g, 4°C, 2 min) then decanted. The precipitate was successively washed with Et_2O and MTBE (1x 25 mL each), and the supernatants were decanted. Residual volatiles were removed under vacuum to provide the title compound (256 mg, 11.6 μmol-4 TFA, quantitative yield) as a white powder.
C18 HPLC purity was determined by ELSD: >99% (RV = 7.65 mL).
Alkyl azide content of the title compound was determined by DBCO titration: 20 μmol/mL by weight, 19.9 μmol/mL by DBCO titration.

[N^{α}-(7-Azido-1,1-dideutero-1-(trideuteromethylsulfonyl)-2-heptyloxycarbonyl)-Lys]$_4$-PEG$_{20kDa}$. C18 HPLC purity was determined by ELSD: 97.2% (RV = 7.65 mL); Alkyl azide content: 20 μmol/mL by weight, 18.6 μmol/mL by DBCO titration.

[N^{α}-(7-Azido-1-cyano-2-heptyloxycarbonyl)-Lys]$_4$-PEG$_{20kDa}$. C18 HPLC purity was determined by ELSD: >99% (RV = 7.83 mL); Alkyl azide content: 20 μmol/mL by weight, 18.3 μmol/mL by DBCO titration.
[N^{α}-(7-Azido-1-cyano-1,1-dideutero-2-heptyloxycarbonyl)-Lys]$_4$-PEG$_{20kDa}$. C18 HPLC purity was determined by ELSD: >96.5% (RV = 7.84 mL); Alkyl azide content: 20 μmol/mL by weight, 20.1 μmol/mL by DBCO titration.

1B. ε-Amino linked Lys-Prepolymer A: [H-Lys[N_3-L(Mod)]-N]}$_4$PEG$_{20kDa}$. The above procedures were also used to prepare prepolymers with the linker carbamate attached to the ε-amine except Boc-Lys-OH was used in the first step.

[N^{ε}-(7-Azido-1-methylsulfonyl-2-heptyloxycarbonyl)-Lys]$_4$-PEG$_{20kDa}$. C18 HPLC purity was determined by ELSD: 93.3% (RV = 7.86 mL); Alkyl azide content: 25 μmol/mL by weight, 27.2 μmol/mL by DBCO titration.

{N^{ε}-[7-Azido-1,1-dideutero-1-(trideuteromethylsulfonyl)-2-heptyloxycarbonyl]-Lys}$_4$-PEG$_{20kDa}$. C18 HPLC purity was determined by ELSD: 95.0% (RV = 7.82 mL); Alkyl azide content: 20 μmol/mL by weight, 22.4 μmol/mL by DBCO titration.

[N^{ε}-(7-Azido-1-cyano-2-heptyloxycarbonyl)-Lys]$_4$-PEG$_{20kDa}$. C18 HPLC purity was determined by ELSD: >99% (RV = 8.13 mL); Alkyl azide content: 20 μmol/mL by weight, 20.6 μmol/mL by DBCO titration.

[N^{ε}-(7-Azido-1-cyano-2-heptyloxycarbonyl)-Lys]$_4$-PEG$_{20kDa}$. C18 HPLC purity was determined by ELSD: 94.4% (RV = 8.10 mL); Alkyl azide content: 20 μmol/mL by weight, 21.4 μmol/mL by DBCO titration.

2. Prepolymer B.

PEG_{20kDa}-[NH-MFCO]$_4$ (Prepolymer B) was prepared as described [4].

3. Amino-microspheres.

Amine-derivatized microspheres were fabricated from Prepolymers A and B using the microfluidic and isolation procedures previously described [4].

4. Fluorescein labeled microspheres

Representative procedure for Fluorescein labeled microspheres.
To limit the likelihood of microbial contamination the follow procedure was done in a HEPA filtered laminar flow hood, and all reagents were filtered through 0.2 μm Nylon-66 filters (Tisch SPEC17984) unless otherwise specified. In a 10 mL syringe, a portion of amino-microsphere slurry in acetonitrile (7 mL, 0.5 mM NH_2, 0.0035 mmol NH_2) was treated with a solution of DIPEA (0.14 mL, 100 mM, 0.014 mmol) in acetonitrile, followed by a solution of 5(6)-FAM-OSu (Thermo Fisher C1311, 0.070 mL, 10 mM, 0.0007 mmol). The suspension was mixed by passage between a second 10 mL syringe connected via a luer coupling. After 20 minutes, to cap unreacted amines, the slurry was treated with a solution of Ac-OSu (500 mM, 0.014 mL, 0.007 mmol) and mixed. After 15 minutes, the slurry was washed with acetonitrile (5 x 6 mL) that had been filtered through a 0.2 um PTFE filter (Sterlitech P/N CPTF0208RR), then finally isotonic pH 5.0 acetate (143 mM NaCl, 10 mM sodium acetate, 0.05% w/v Tween, 5 x 5 mL) that had been filtered through a 0.2 um PES filter (Sterlitech P/N CPESO2O8RR). The slurry was pelleted at 3000 RCF for 5 – 10 minutes in between washes, and was loaded into 0.3cc insulin syringes with an integral 29G x ½" needle (BD 324702) for subcutaneous injections into rats.

5. Fluorescein labeled hydrogel cones

Representative procedure for Fluorescein labeled microspheres.
To a solution of Prepolymer A in (18 mM -NH_2, 0.250 mL, 0.0045 mmol) in 20 mM pH 5.0 acetate, 0.092 mL of pH 8.5 HEPES (200 mM) was added, followed by a solution of 5(6)-FAM-OSu (10 mM, 0.047 mmol). After 15 min a solution of Ac-OSu (500 mM, 0.019 mL) in DMF was added then after 15 minutes water (0.042 mL) was added. This gives a solution containing 10 mM crosslinkable azide end group. Immediately this solution was mixed with an equal volume (0.450 mL) of Prepolymer B (10 mM) and place into Eppendorf tubes (0.100 mL per tube). After curing for 1.5 hours, the resulting hydrogel cones were transferred to 50 mL of 10 mM pH 5.0 acetate, then stored at 4 ^oC prior to use in degelation assays.

6. [Gln^{28}]Exenatide releasing and fluorescein labeled [Gln^{28}]exenatide releasing microspheres

Amino-microspheres were derivatized with MFCO and loaded with azido-linker(mod)-[Gln^{28}] exenatide as described [5]. Cleavable hydrogel crosslinks contained either the –CN or $(MeOCH_2CH_2)_2NSO_2$- modulators. The fluorescein labeled version of these microspheres were made using a modification of the reported procedure given below.

Exemplary procedure for [Gln^{28}]exenatide releasing / fluorescein labeled microspheres.

A solution of 6-azidohexanoyl-aminoacetamido fluorescein (1.8 μmol) in MeCN (0.2 mL) was added to a slurry of MFCO derivatized microspheres [5] (4.5 mL) containing 9.6 μmol of MFCO.

The reaction mixture was mixed by rotation at ambient temperature for 18 hr then a solution of N^{α}-(7-Azido-1-cyano-2-heptyloxycarbonyl)-[Gln^{28}]exenatide [5] (8.2 umol) in water (3.2 mL) was added, and mixing was allowed to continue for another 18 hr. The microsphere slurry was purified and exchanged into isotonic acetate dosing buffer (pH 5.0, 10 mM Na Acetate, 143 mM NaCl, 0.05% w/v Tween 20) as previously described [5].

III. In vitro characterization of hydrogels and microspheres

1. Reverse gelation (t_{RG}) assay for bulk gel cones and microspheres

The time to complete solubilization or reverse gelation time (t_{RG}) of fluorescein-labeled microspheres and bulk gel cones was performed spectrophotometrically in mesh-divided cuvettes as previously described [3]. Samples were immersed in buffer at pH 8.4 and 9.0 (bicine / borate) for fast-degrading gels ($t_{RG} \leq 250$ hours) or pH 9.0 and 9.4 (borate) for slower - degrading gels ($t_{RG} \geq 250$ Hours). Absorbance was continuously monitored at 495 nm while cuvettes were maintained at 37 °C until a constant maximal A_{495} was reached. The t_{RG} is determined as the time of intersection of the steepest part of the degelation curve with the horizontal line representing total delegation as shown in **Figure 2A** of the main text.

IV. In vivo characterization of hydrogel-microspheres

1. Microsphere injections and harvesting of tissue.

For each fluorescein-labeled microsphere formulation, three female Sprague Dawley rats (200-250 g), each destined to carry 8 time points of SC injections, were anesthetized with isoflurane gas and shaved on their back. The intervals for injections of each animal were calculated as ($t_{RG\_in\ vitro}$ x 3)/8. At each time point, 100 uL of microsphere slurry was injected SC into one of 8 sites of a rat (n=3) equally spaced over each side of its back. After every other injection, the location of each was marked with a circular tattoo ~12 mm in diameter.

Following the final injection, rats were euthanized with CO_2 and their hair was removed by shaving and treatment with Nair (Church & Dwight). Each site of injection was palpated for presence of microspheres, then imaged by ultrasound (Visual Sonics VIVO 770) and, when specified, measured with calipers. The tissue containing the implant was then excised down to the peritoneal membrane using a 12 mm diameter biopsy punch (Acuderm Acu.Punch P1250). Tissue samples were placed into 1.5 mL Eppendorf tubes and stored at -80 ^{o}C prior to processing for fluorescein measurements.

2. Measurement of subcutaneous microsphere implants.

Calipers. The two longest perpendicular axes (length and width) in the x/y plane of each implant were measured to the nearest 0.1 mm using a digital Vernier caliper by an observer familiar with collecting caliper measurements of xenograft tumors. The depth was assumed to be equivalent to the shorter of the perpendicular axes, y, and volumes were calculated as $xy^2/2$ [6].

Ultrasound. The implants were imaged using a VisualSonics Vevo 2100 ultrasound instrument, using a 13-24 MHz transducer (Fujifilm VisualSonics MS250), and Aquasonic 100 ultrasound gel. The probe was mounted on a motorized linear actuator controlled by the instrument's software and used to acquire 2D cross sectional B-mode images in 0.5 mm steps for a distance of ~6- to 20 mm that included ~2 mm of normal tissue on either side of the

implant. This produced a stack of 2D images containing the implant, that are converted to a 3D model of the implant in the instrument's software. The implant area in each image was determined by selecting the echolucent area that was distinct from the surrounding tissue. The boundary of the implant was drawn onto the images and the implant volume was determined by integration using VisualSonics software.

Gel mass measurements. After thawing to ambient temperature, tissue samples were digested with 1.0 mL of 1 N NaOH at 70 ^{o}C for 20 minutes, vortexed at moderate speed, then pelleted at 20000 RCF for 10 minutes. Then 0.15 mL of each of the digested samples was transferred to a well of a solid black microtiter plate (Greiner Bio One, 655209). Fluorescein fluorescence was then quantified using a microplate reader (Spectrum i3, Molecular Devices; ex 485 nm, em 535 nm). For HPLC analysis, 100 uL of the tissue digest was neutralized with 7 uL of AcOH, followed by addition of 200 uL of ACN/MeOH/TFA (1:1:0.005); after centrifugation at 20,000 RCF, 10 uL of the supernatant was analyzed by HPLC using fluorescence detection (ex = 441 nm, em = 521 nm).

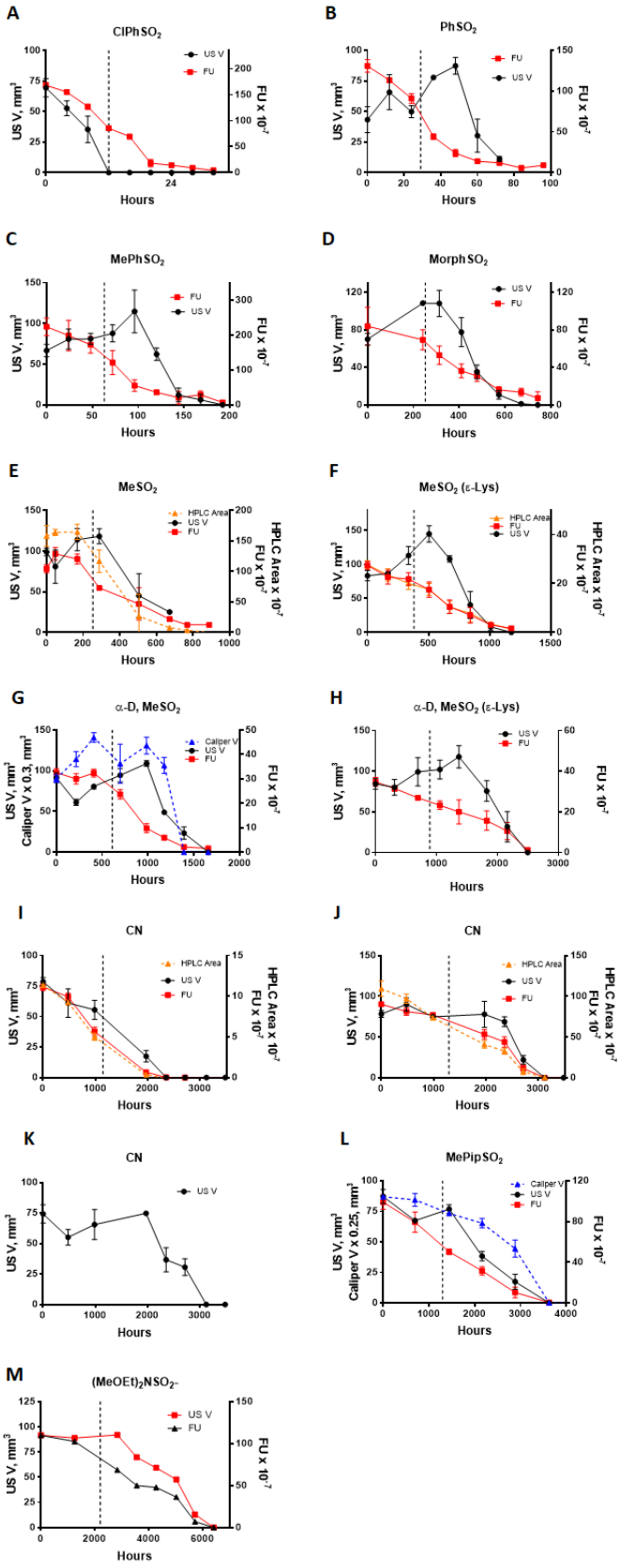
A
ClPhSO2
US V
FU
US V, mm3
FU x 10-7
Hours
B
PhSO2
C
MePhSO2
D
MorphSO2
E
MeSO2
HPLC Area
HPLC Area x 10-7
F
MeSO2 (ε-Lys)
G
α-D, MeSO2
Caliper V x 0.3, mm3
H
α-D, MeSO2 (ε-Lys)
I
CN
J
CN
K
CN
L
MePipSO2
Caliper V x 0.25, mm3
M
(MeOEt)2NSO2-

Figure S1. In vivo degradation and volume changes of hydrogel microspheres with different cross-linker half-lives. Vertical dashed lines indicate the in vitro t_{RG} of the microspheres. Measurements shown include: ultrasound determined volume (US), caliper measured volume (Caliper V), and gel mass as determined by fluorescein in tissue extracts by the plate reader method (FU) or the HPLC method (HPLC area). **A,B,C,D,E,G,I,J,K,L** and **M** show data from gels containing crosslinks to the α-amine of Lys and a hydrogen atom adjacent to the modulator, gels **F** and **H** have crosslinks to the ε-amine of Lys, and gels **G** and **H** contain a deuterium atom adjacent to the modulator (see also **Table S1** for an explanation of modulators and crosslinks). **I, J** and **K** have the same crosslinker containing the –CN modulator but differ in their payload: **I** simply contains the fluorescein label used to track degradation, **J** and **M** contain, in addition to the fluorescein probe, a releasable peptide drug [Gln^{28}]exenatide [5], and **K** that lacks the fluorescein probe but contains releasable [Gln^{28}]exenatide.

Table S1. ***In vitro*** t_{RG} and crosslinker cleavage $t_{1/2}$ values for hydrogels studied here.

Entry in Figure S1	Modulator	Alpha atom	$t_{1/2,L2\ invitro}$ (hours)[a]	Amine of lysine	Fluorescein label	Releasable peptide	$t_{RG\ in\ vitro}$ as a bulk gel cone (hours)	$t_{RG\ in\ vitro}$ as microspheres (hours)	Gel Quality Factor (f)
A	$ClPhSO_2$-	H	36	α	Yes	No	16 ± 5	12 ± 0.9	0.5086
B	$PhSO_2$-	H	71	α	Yes	No	30 ± 3.7	29 ± 1.9	0.4824
C	$MePhSO_2$-	H	150	α	Yes	No	63 ± 1.3	62 ± 3.2	0.4806
D	$MorphSO_2$-	H	250[b]	α	Yes	No	190 ± 11	260 ± 15	0.1981
E	$MeSO_2$-	H	250	α	Yes	No	250 ± 33	253 ± 15	0.2135
F	$MeSO_2$-	H	427	ε	Yes	No	360 ± 28	380 ± 20	0.2773
G	$MeSO_2$-	D	450	α	Yes	No	570 ± 70	610 ± 60	0.0020
H	$MeSO_2$-	D	950	ε	Yes	No	840 ± 26	890 ± 51	0.2534
I	-CN	H	1200[b]	α	Yes	No	1050 ± 63	1150 ± 49	0.2422
J	-CN	H	1200[b]	α	Yes	Yes	ND	1290 ± 130	0.1784
K	-CN	H	1200[b]	α	NO	Yes	ND	ND	ND
L	$MePIPSO_2$-	H	1560[b]	α	Yes	No	1180 ± 15	1430 ± 190	0.2638
M	$(MeOCH_2CH_2)_2NSO_2$-	H	2660[b]	α	Yes	Yes	ND	2750 ± 230	0.2015

[a] reported in [7], the first order rate constant for linker cleavage $k_{L2,in\ vitro} = Ln(2)/t_{1/2,L2\ in\ vitro}$.
[b] revised $t_{1/2}$ using the reported method [7].

SI References

(1) Santi, D.V. ; Schneider, E.L.; Ashley, G.W. Macromolecular prodrug that provides the irinotecan (CPT-11) active-metabolite SN-38 with ultralong half-life, low C(max), and low glucuronide formation. *Journal of medicinal chemistry*, **2014**, *57*, 2303-2314.

(2) Ashley, G.W.; Henise, J.; Reid, R.; Santi, D.V. Hydrogel drug delivery system with predictable and tunable drug release and degradation rates. *Proc Natl Acad Sci U S A* 110 **2013**, *110*, 2318-2323.

(3) Henise, J.; Hearn, B.R.; Ashley, G.W.; Santi, D.V. Biodegradable tetra-PEG hydrogels as carriers for a releasable drug delivery system. *Bioconjugate Chemistry* **2015**, *26*, 270-278.

(4) Schneider, E.L.; Henise, J.; Reid, R.; Ashley, G.W.; Santi, D.V. Hydrogel drug delivery system using self-cleaving covalent linkers for once-a-week administration of exenatide. *Bioconjugate Chemistry* **2016**, *5*, 2010-2015.

(5) Schneider, E.L.; Hearn, B.R.; Pfaff, S.J.; Fontaine, S.D.; Reid, R.; Ashley, G.W.; Grabulovski, S.; Strassberger, V.; Vogt, L.; Jung, T.; Santi, D.V. Approach for Half-Life Extension of Small Antibody Fragments That Does Not Affect Tissue Uptake. *Bioconjugate Chemistry* **2016**, DOI: 10.1021/acs.bioconjchem.1026b00469.

(6) Tomayko, M.M.; Reynolds, C.P. Determination of subcutaneous tumor size in athymic (nude) mice. *Cancer chemotherapy and pharmacology* **1989**, *24*, 148-154.

(7) Santi, D.V.; Schneider, E.L.; Reid, R.; Robinson, L.; Ashley, G.W. Predictable and tunable half-life extension of therapeutic agents by controlled chemical release from macromolecular conjugates. *Proc Natl Acad Sci U S A* **2012**, *109,* 6211-6216**.**